European Journal of Medicinal Chemistry 56 (2012) 400–408

Contents lists available at SciVerse ScienceDirect

European Journal of Medicinal Chemistry

journal homepage: http://www.elsevier.com/locate/ejmech

Short communication

Anticancer siRNA delivery by new anticancer molecule: A novel combination strategy for cancer cell killing☆

Prathap Reddy Muktapuram [a,1], Rishi Kumar Gara [b,1], Komal Sharma [a], Chilappa Rohit [c], Kolupula Srinivas [c], Durga Prasad Mishra [b], Surendar Reddy Bathula [a,*]

[a] Division of Pharmaceutics, CSIR-Central Drug Research Institute, Chattar Manzil Palace, 1-M.G. Marg, Lucknow 226001, India
[b] Endocrinology Division, CSIR-Central Drug Research Institute, Lucknow 226001, India
[c] Medicinal Chemistry, National Institute of Pharmaceutical Education and Research (NIPER-Hyderabad), Balanagar, Hyderabad 500037, India

ARTICLE INFO

Article history:
Received 17 April 2012
Received in revised form
17 July 2012
Accepted 18 July 2012
Available online 27 July 2012

Keywords:
Anticancer molecule
Anticancer siRNA
Combination therapy
Survivin gene

ABSTRACT

The present report describes development of a novel, bifunctional molecule possessing both selective antiproliferative activity and siRNA transfection ability. We synthesized a series of cationic lipobenzamides and screened for *in vitro* anticancer activities against a panel of cancer and non-cancer cells. The molecule with a ten carbon chain-length (C10M) significantly inhibited proliferation of cancer cells via arresting the cell cycle predominantly in the G1 phase; but did not affect non-cancerous cells. C10M effectively mediated siRNA delivery *in vitro*. The combined anticancer effect of the delivery of C10M together with its survivin-targeting siRNA cargo was significantly ($p < 0.05$) superior to that of agent alone. To our knowledge, this is the first report of a dual-purpose molecule with intrinsic anticancer activity and suitability for use in siRNA delivery.

1. Introduction

RNA interference (RNAi), an evolutionarily conserved ubiquitous gene silencing mechanism, has potential for clinical development of nucleic acid therapeutics [1]. Recently, several new RNAi-based drugs have been translated into clinical testing [2]. The delivery vector is crucial for clinical success of therapeutic RNAi [3]. To fully exploit the therapeutic potential of RNAi in cancer therapy, various small interfering RNA (siRNA) delivery strategies have been developed, including stable nucleic acid-lipid particles (SNALP) formulations that encapsulate siRNA designed to silence polo-like kinase 1(PLK1) [4], siRNA–lipoplexes made up of cationic lipid AtuFECT01® and siRNA against protein kinase N3(PKN3) [5], cyclodextrin nanoparticle carriers of siRNA for solid tumors (CALAA-01) [6], siRNA in complex with anionic liposomes [7], self assembled liposome–polycation–DNA (LPD) nanoparticles [8], cationic lipids [9], and chemically modified siRNAs [10].

These siRNA delivery strategies are based on single agent therapies, but combinational therapy is more effective when compared to a single agent in curing cancer [11]. Developing a selective antiproliferative agent which can deliver siRNA is challenging but has great potential toward the development of siRNA mediated therapeutic intervention in cancer.

PEG coated polymeric nanoparticles are the most promising nonviral vectors for systemic delivery of siRNA [12]. PEGylation not only reduces the toxicity of cationic lipids (CL) and cationic polymers such as polyethyleneimine (PEI) but also inhibits particle aggregation [13]. Self-assembled, LPD (liposome–polycation–DNA complex) is a potent nanocarrier for systemic delivery of siRNA [14]. In a recent study we have shown that lipid–polycation–DNA (LPD) nanoparticles fabricated using an apoptosis-promoting cationic lipid, DSGLA (*N*,*N*-distearyl-*N*-methyl-*N*-2[*N*′-(N^2-guanidino-L-lysinyl)] aminoethyl ammonium chloride), significantly inhibited tumor growth in comparison to LPD constructed using the known cationic lipid, 1,2-di-(9Z-octadecenoyl)-3-trimethylammonium-propane (DOTAP) [15]. In another study, we explored the potential of DSAA (*N*,*N*-distearyl-*N*-methyl-*N*-2-(*N*′-arginyl) aminoethyl ammonium chloride); a cationic lipid structurally similar to DSGLA in overcoming drug resistance in tumors [16]. The LPD nanoparticles containing either DOTAP (DOTAP-LPD) or DSAA (DSAA-LPD) efficiently delivered myelocytomatosis cellular oncogene (c-Myc) siRNA into melanoma cells. However, tumor growth inhibition was more prominent with DSAA-LPD nanoparticles.

☆ CDRI Communication No-8288 2.

* Corresponding author. Tel.: +91 522 2612411x4358; fax: +91 522 2623405.
E-mail address: bsreddy@cdri.res.in (S.R. Bathula).

[1] These two authors contributed equally.

0223-5234/$ – see front matter © 2012 Elsevier Masson SAS. All rights reserved.
http://dx.doi.org/10.1016/j.ejmech.2012.07.035

Interestingly, co-administration of Paclitaxel (PTX) and DSAA-LPD completely inhibited the B16F10 tumor [17]. These studies demonstrate the importance of a potentially bioactive lipid as a delivery vector possessing intrinsic therapeutic activity.

The objective of this study was to design a bifunctional molecule that can selectively kill cancer cells and deliver anticancer siRNA. N-(2-Dialkylaminoalkyl)-substituted benzamides are important class of bioactive small molecules with a wide range of biological activities such as anti-emetic (Metoclopramide) and anti-psychotic (Tiapride); and have also been extensively investigated as diagnostic probes for malignant melanoma and sigma receptor targeting ligands [20]. Melanin-targeted, radioiodinated benzamides such as N-(2-diethylaminoethyl)-4-iodobenzamide (BZA) and N-(2-diethylaminoethyl)-3-iodo-4-methoxybenzamide (IMBA) showed promise as tumor-imaging agents in pre-clinical studies for the scintigraphic detection of melanoma [21]. Earlier we have reported that the conjugation of an eight carbon twin chain cationic lipid moiety to 17β-estradiol generated a new antiproliferative agent that significantly inhibits the proliferation of breast cancer cells independent of estrogen receptor expression, without harming normal cells [18]. In a separate study Pal and co-workers developed a new class of cationic lipid-conjugated haloperidol derivatives [19]. However, nucleic acid delivery to cytosol was not reported for these classes of molecules.

We hypothesized that synthesis of cationic N-(2-dialkylaminoalkyl)-substituted benzamides with a medium-length alkyl chain (C7–C12) might yield a new anticancer molecule with siRNA delivery potential. Toward this goal, we have synthesized a series of [2-(4-methoxy-benzoylamino)-ethyl]-methyl-dialkyl-ammonium iodides with varying number of side chain carbon atoms starting from two to eighteen carbons and evaluated as selective anticancer agents against four human cancer cell lines and four noncancer cell lines. Further we have tested the *in vitro* siRNA delivery efficacy of most active cationic lipo-benzamide, C10M by tracking uptake of fluorescein labeled-siRNA in DU-145 cells. Finally we have studied the combined anticancer effect of both the antiproliferative lipo-benzamide C10M and anticancer siRNA, using siRNA targeting to the survivin gene. Survivin is an anti-apoptotic protein that is basally-expressed in normal tissue and overexpressed in nearly all human cancers. The expression of survivin in tumor cell lines increases with proliferation rate and resistance to therapy. Survivin is therefore a potential target for the development of novel anticancer therapies. It is also known from the literature that knockdown of survivin expression results tumor growth inhibition [22].

2. Results and discussion

2.1. Chemistry

The structures and general synthetic strategies adopted for preparing cationic benzamide derivatives are outlined in Scheme 1. The distinctive novel structural features common to the cationic benzamide derivatives reported here include: (a) The presence of hydrophobic groups which are directly linked to the positively charged nitrogen atom and (b) the presence of 4-methoxybenzamide group. As shown in Scheme 1, anisoylchloride reacted with mono-Boc-protected ethylenediamine to generate *tert*-butyl(2-(4-methoxybenzamido)ethyl)-carbamate. Boc deprotection of the anisamide derivative using TFA/DCM followed by alkylation with K_2CO_3/respective alkyl bromide offered the twin chain tertiary amine intermediates with C2–C18 carbon atoms. Subsequent quaternization of nitrogen with methyl iodide resulted in the formation of target cationic methoxybenzamide amphiphiles. All compounds were characterized using ^{1}H NMR and mass spectrometry. The purity of these compounds was ascertained by TLC, ^{13}C NMR, HRMS and differential scanning calorimetry in case of C10M (Fig. S2). The % purity of all analogs was confirmed by HPLC (Fig. S3) as ≥96%.

2.2. Biological experiments

2.2.1. Cytotoxicity studies

Novel cationic benzamide derivatives with varying number (C2–C18) of side chain carbon atoms namely C2M–C18M were evaluated for *in vitro* anticancer activity using a CCK-8 assay across different molar concentrations (0.5, 1, 2.5, 5, 10, 20 μM). Briefly, cells ($3–5 \times 10^3$ cells/well) were cultured in 96 well tissue culture plates and treated with different concentrations of benzamide derivatives for 48 h. At the end of incubations, 10 μL of CCK-8 solution was added to each well and incubated for 3 h. Absorbance was recorded at 540 nm using Fluostar Omega spectrofluorimeter (BMG Labtech, Offenburg, Germany). The growth-inhibitory effects were studied in four human cancer cell lines, DU-145 & PC-3 (Human prostate cancer cells), MCF-7 (breast adenocarcinoma), HepG2 (hepatocellular carcinoma) and four non-cancer cell lines, WPMY-1 (prostate), HEK-293 (Human embryonic kidney), COS-7 (African green monkey kidney), NIH/3T3 (mouse embryo fibroblast) in order to determine their cyto-selective nature. The results are presented in Table 1. IC_{50} values were based on dose–response curves. Compounds with medium-length alkyl chains (C7–C12) displayed a concentration-dependent cytotoxic profile in all four cancer cell lines. Among the benzamides, C10M significantly inhibited the proliferation of all four cancer cells at all concentrations (IC_{50} range from 3.59 to 8.12 μM) without affecting the normal cells. The compounds having IC_{50} value more than 20 μM, were considered inactive.

2.2.2. Lipo-benzamide derivative with ten-carbon chain (C10M) induces apoptosis

We first considered induction of apoptosis as a mechanism whereby C10M could kill cancer cells. We performed the Annexin V/Propidium iodide (PI) binding assay to quantitatively differentiate between apoptotic and necrotic cells. For this experiment, cells were treated with 5 μM C10M for 24 h and harvested in PBS

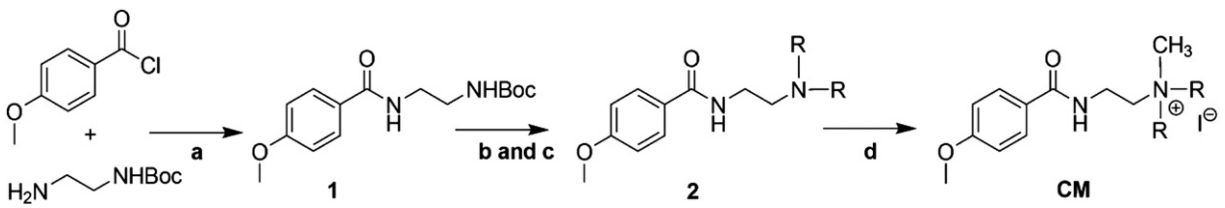

Scheme 1. Outlines the synthetic strategy employed for preparing the novel cationic lipo-benzamides described in the present investigation. (a) Triethylamine, THF, rt, 5 h (b) TFA and DCM (1:1), rt, 1.5 h (c) R–Br, ethyl acetate, K_2CO_3, 70 °C, 12 h (d) DCM, CH_3I, rt, 3 h. For C2M: R = C_2H_5, C3M: R = C_3H_7, C4M: R = C_4H_9, C5M: R = C_5H_{11}, C6M: R = C_6H_{13}, C7M: R = C_7H_{15}, C8M: R = C_8H_{17}, C9M: R = C_9H_{19}, C10M: R = $C_{10}H_{21}$, C11M: R = $C_{11}H_{23}$, C12M: R = $C_{12}H_{25}$, C13M: R = $C_{13}H_{27}$, C14M: R = $C_{14}H_{29}$, C15M: R = $C_{15}H_{31}$, C16M: R = $C_{16}H_{33}$, C17M: R = $C_{17}H_{35}$ and C18M: R = $C_{18}H_{37}$.

Table 1
Anticancer activity (IC_{50}, μM) of novel lipo-benzamides.

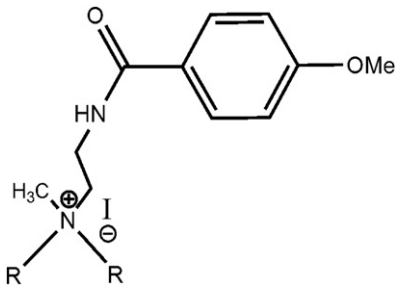

Compound	R	Cells originated from cancer tissue				Cells originated from non-cancer tissue			
(IC_{50} μM)		HepG2	PC-3	MCF-7	DU-145	COS-7	NIH/3T3	HEK-293	WPMY-1
C2M	C_2H_5	>20	>20	>20	>20	>20	>20	>20	>20
C3M	C_3H_7	>20	>20	>20	>20	>20	>20	>20	>20
C4M	C_4H_9	>20	>20	>20	>20	>20	>20	>20	>20
C5M	C_5H_{11}	>20	>20	>20	>20	>20	>20	>20	>20
C6M	C_6H_{12}	>20	>20	>20	>20	>20	>20	>20	>20
C7M	C_7H_{15}	5.449	17.63	>20	10.38	>20	1.596	>20	>20
C8M	C_8H_{17}	8.679	11.91	>20	15.45	>20	2.199	>20	>20
C9M	C_9H_{19}	>20	>20	>20	>20	>20	16.69	>20	>20
C10M	$C_{10}H_{21}$	5.309	3.645	7.55	3.957	>20	18.14	>20	>20
C11M	$C_{11}H_{23}$	>20	>20	>20	7.539	>20	6.659	>20	>20
C12M	$C_{12}H_{25}$	>20	>20	>20	11.39	>20	11.34	>20	>20
C13M	$C_{13}H_{27}$	13.86	>20	>20	6.830	>20	7.67	>20	>20
C14M	$C_{14}H_{29}$	>20	>20	>20	10.41	>20	12.18	>20	>20
C15M	$C_{15}H_{31}$	>20	>20	>20	>20	>20	>20	>20	>20
C16M	$C_{16}H_{33}$	>20	>20	>20	>20	>20	>20	>20	>20
C17M	$C_{17}H_{35}$	>20	>20	>20	>20	>20	>20	>20	>20
C18M	$C_{18}H_{37}$	>20	>20	>20	>20	>20	>20	>20	>20

and analyzed using a flow cytometer. Dual staining clearly discriminated between early apoptotic (Annexin positive), late apoptotic (dual positive) and necrotic (only PI positive) cells [23]. As can be seen in Fig. 1a, exposure to C10M resulted in increased percentage of early apoptotic cells from 3% in the untreated control group to 23% in the treated group in DU-145 cells. In case of PC-3 cells as well, C10M increased the percentage of both early and late apoptotic cells in comparison to the untreated control. Early apoptotic cells rose from 1% in the untreated group to 51.48% in C10M-treated group. Late apoptotic cells increased from 1% to 21.49% in untreated and treated groups respectively. In the non-cancerous WPMY-1 cells, C10M treatment did not increase the number of apoptotic cells in comparison to the untreated control (Fig. 1a). These observations demonstrate that C10M induces apoptosis in cancer cells but not in cells of non-cancer origin.

2.2.3. Effect of lipo-benzamides on cell cycle progression

We also independently evaluated whether arrest of cell cycle progression could be a mechanism of antiproliferative activity of the lipo-benzamides. Cancer cells (PC-3, DU-145 & HEK-293) treated with 5 μM each of compounds C7M, C8M, C9M, C10M, C11M and C12M for 24 h were permeabilized, stained with PI and subjected to flow cytometric analysis. Histograms of flow cytometric data are shown in Fig. 1b–d. The histograms were quantitatively analyzed using a curve-fitting program to determine the percentage of cells in each of the G0/G1, S, and G2/M phases. Consistent with the results obtained in the cell proliferation and apoptosis induction assays, C10M significantly caused G0/G1 phase arrest with induction of extensive apoptosis in PC-3 cells. In Fig. 1b, cells in the G0/G1 phase increased from 44.20% in controls to 53.83%, 62.97%, 54.06%, 69.49%, 50.20% and 50.81%, after treatment with C7M, C8M, C9M, C10M, C11M and C12M respectively. While 5 μM of other lipo-benzamides did not significantly affect the phase distribution of the cell cycle in DU-145 cells, C10M triggered a significant increase of cells in the sub-G0 phase (Fig. 1c). In case of non-cancer cells HEK-293, (Fig. 1d) C8M and C10M had measurable effects on the phase distribution of the cell cycle. The above results demonstrate that the apoptosis inducing ability of C10M in cancer cells correlates with its ability to arrest the cell cycle in the G0/G1 phase. Further experiments are needed and work is in progress to address the significance of the observation that the extent of apoptosis induction and cell cycle arrest differ in the case of DU-145 and PC-3 cells.

2.2.4. Molecular docking studies

In this study, we demonstrated that among the structurally similar lipo-benzamides, C10M induced significant growth inhibition of all the tested human cancer cells (Table 1). We observed induction of apoptosis in C10M treated prostate cancer cells and G0/G1 phase arrest in C10M treated PC-3 cells. It is well known that regulation of the cell cycle involves series of tightly integrated events, involving cyclins and cyclin-dependent kinases (CDKs); and inhibition of the above proteins cause cell cycle arrest [24–26]. It is also reported that CDK2 inhibition causes G0/G1 phase arrest [27]. We therefore attempted to dock C7M through C12M in the active site of the human CDK2 protein structure (Pdb ID: 1CKP). Glide flexible docking simulations were performed using Glide, version 5.5 [28]. The results are presented in Table 2. Molecular docking results indicate that C10M has stronger binding affinity (Glide score −1.6 kcal/mol) compared to its analogs (C7M–C9M, C11M & C12M). These results are consistent with experimental observations of the extent of cell cycle arrest induced by this series of compounds. The theoretical binding mode of the protein–ligand interactions in respect of C10M is presented in Fig. 1e, which suggests hydrogen bonding interactions with Asn 136 and Lys 291. The *in silico* study gives an insight about the molecular level interactions.

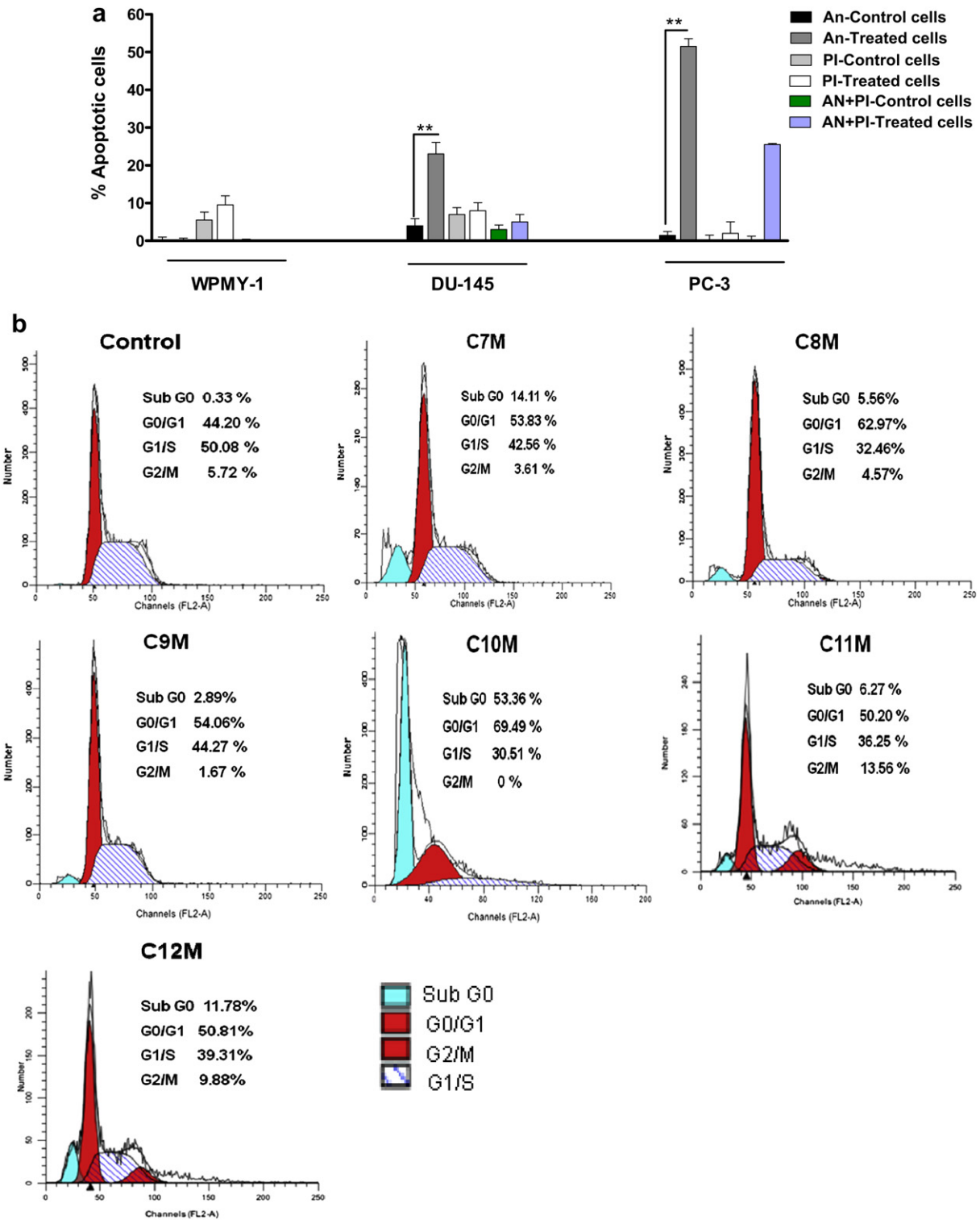

Fig. 1. a). Flow cytometry was done for detection of apoptosis in DU-145, PC-3 and WPMY-1 cells after treatment with 5 μM of C10M for 24 h. Treated cells were trypsinized and washed with PBS, and apoptosis studies were performed by annexinV-FITC kit as per manufacturer's instructions. Stained cells were analyzed by FACScan flow cytometer (Becton Dickinson, USA). All the experiments were performed at least three times. Values are expressed as mean ± SEM of two independent experiments performed in duplicate. The difference in the data obtained between An-control and An-treated cells is statistically significant in both DU-145 and PC-3 cells ($^{**}p < 0.001$), whereas in WPMY-1 cells difference in the data is statistically insignificant ($p < 0.26$). b). Cell cycle profiles of 5 μM of C7M, C8M, C9M, C10M, C11M and C12M treated PC-3 cell. For cell cycle analysis cells were fixed in 70% ethanol at −20 °C for 1 h, washed twice with PBS and treated with 1 mg/mL RNase for 30 min at 37 °C. Cellular DNA was stained with 50 μg/mL PI in PBS. Stained cells were analyzed by FACScan flow cytometer (Becton Dickinson, USA). All the experiments were performed at least three times. c). Cell cycle analysis of DU-145 cells treated with 5 μM of C7M, C8M, C9M, C10M, C11M and C12M compounds. Untreated cells (blank) were used as control. d). Effect of antiproliferative lipo-benzamides such as C7M, C8M, C9M, C10M, C11M and C12M on the cell cycle of, non-cancerous, HEK-293 cell line. Cells were incubated in the presence of the lipo-benzamide compounds for 24 h. Aliquots of cells were taken in duplicate for cell cycle analysis by flow cytometry using propidium iodide staining. The data are the average of two separate experiments using different batches of cells. e). Docking pose of C10M molecule in the active site of CDK2 target (Pdb ID: 1CKP). C10M is depicted in ball and stick model. The key H-bond interactions between the compounds and the residues of the binding pocket are highlighted as dotted lines.

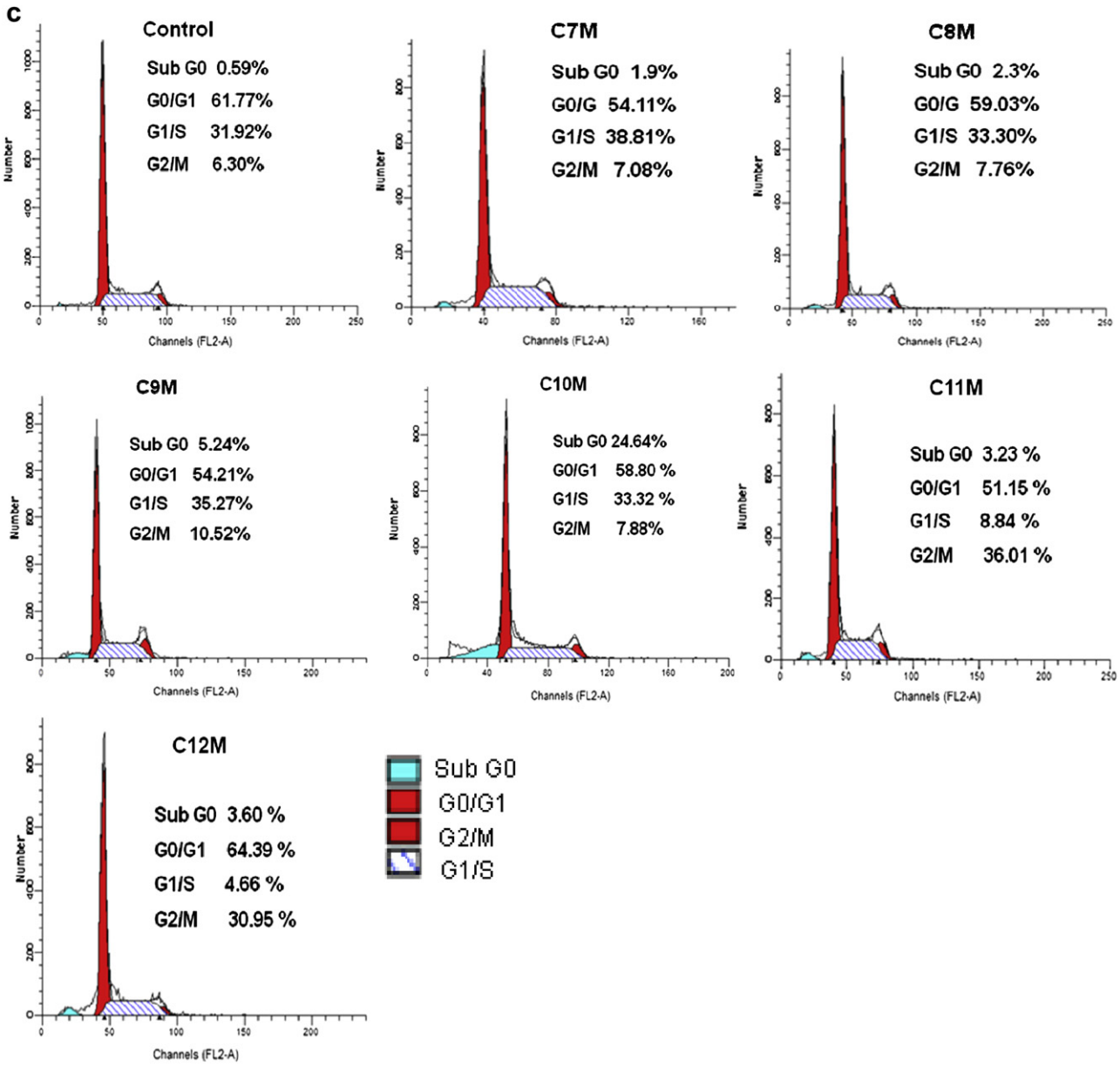

Fig. 1. (*continued*).

2.3. Transfection biology

We tested the efficiency of siRNA delivery of the selective antiproliferative agent C10M in DU-145 cells by tracking uptake of fluorescein labeled-siRNA (F-siRNA). We also measured the combined anticancer efficacies of both the anticancer lipid and anti-survivin siRNA in these cells. For that we prepared self-assembled C10M nanostructures by two stage ethanol injection. In the first step, 2.5 mg of C10M was dissolved in 125 μL of absolute ethanol and the entire ethanol solution of C10M was added rapidly to 250 μL of 5% mannitol solution in a 1.5 mL centrifuge tube. The aqueous phase immediately turned milky as a result of self-assembly. In the next stage, 74 μL of the above milky aqueous phase was rapidly injected into 926 μL of 5% mannitol solution to prepare cationic vesicles of the antiproliferative lipo-benzamide. The 1 mM formulation thus prepared was stable for three days at ambient temperature, but the compound slowly precipitated thereafter (data not shown). The above formulation was used in all further experiments without removing ethanol.

We measured the hydrodynamic diameters of self-assembled C10M nanostructures alone or as siRNA/C10M complexes to further characterize them. Strikingly, the sizes of C10M/siRNA complexes varied within a narrow range (200–240 nm) across the entire series of lipid/siRNA ratios and was smaller as compared to self assembled C10M (Table S1). This decrease in size of complexes than C10M indicates the siRNA compacting efficacy of C10M.

2.3.1. Cellular uptake of C10M/siRNA complexes

The efficiency of intracellular siRNA delivery by self-assembled C10M was evaluated by tracking uptake of fluorescein labeled-siRNA (F-siRNA) in DU-145 cells by flow cytometry. For this study, 1 μg of F-siRNA diluted to 100 μL with Roswell Park Memorial Institute (RPMI) culture medium was complexed with varying

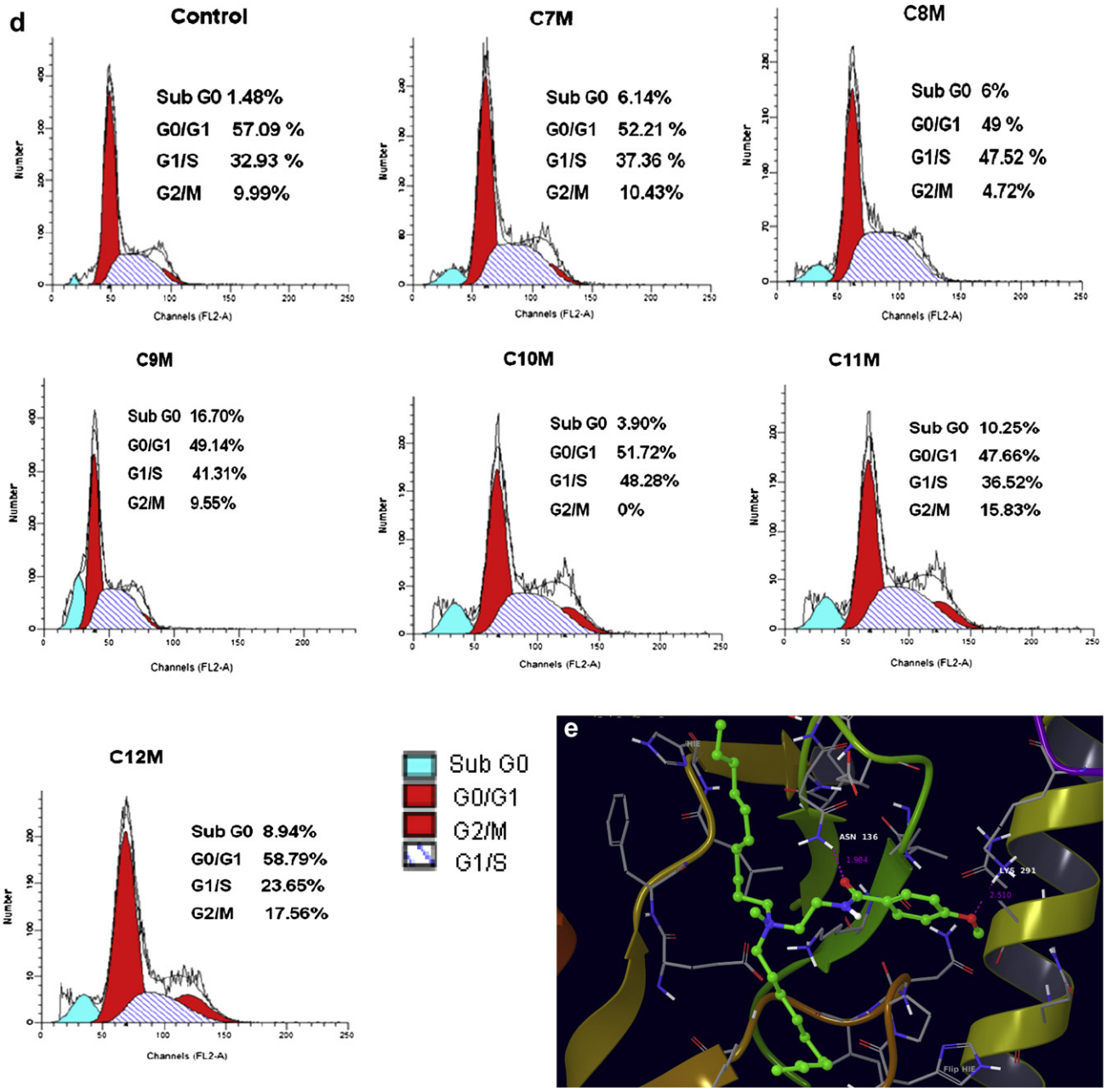

Fig. 1. (*continued*).

amounts of C10M cationic vesicles (1:5, 1:10, 1:20, 1:25 weight ratio) diluted to 100 μL with RPMI and incubated for 30 min. The resultant C10M/siRNA complexes and free F-siRNA was further diluted with 300 μL of RPMI containing 10% FBS to prepare 500 μL of lipoplex. DU-145 cells seeded in 6 well plates were incubated with the lipoplex for 12 h. After incubation, cells were washed twice with PBS and analyzed by flow cytometry. Results of cellular uptake of uncomplexed siRNA as well as C10M complexed fluorescein-labeled siRNA in DU-145 cells are summarized in the bar graph in Fig. 2a and the fluorescence intensity distribution histograms are presented in Fig. S1. Free siRNA, as expected, exhibited very poor uptake efficiency presumably due to the repulsive interactions between negatively charged siRNA and the negatively charged cell membrane. After complexation with C10M higher F-siRNA uptake efficiency was observed and it was further increased with increasing lipid concentration. It is evident from the above results that the cationic benzamide could efficiently deliver siRNA to the tumor cells and the delivery was concentration dependent.

Table 2
Molecular docking scores of molecules C7M–C12M into the active site of CDK2 target (Pdb ID: 1CKP).

Molecule no.	Glide score (kcal/mol)
C10M	−1.6
C8M	−0.8
C7M	−0.3
C9M	1.5
C12M	1.6
C11M	2.1
Reference (Co-crystallized ligand: Purvalanol B)	−1.8

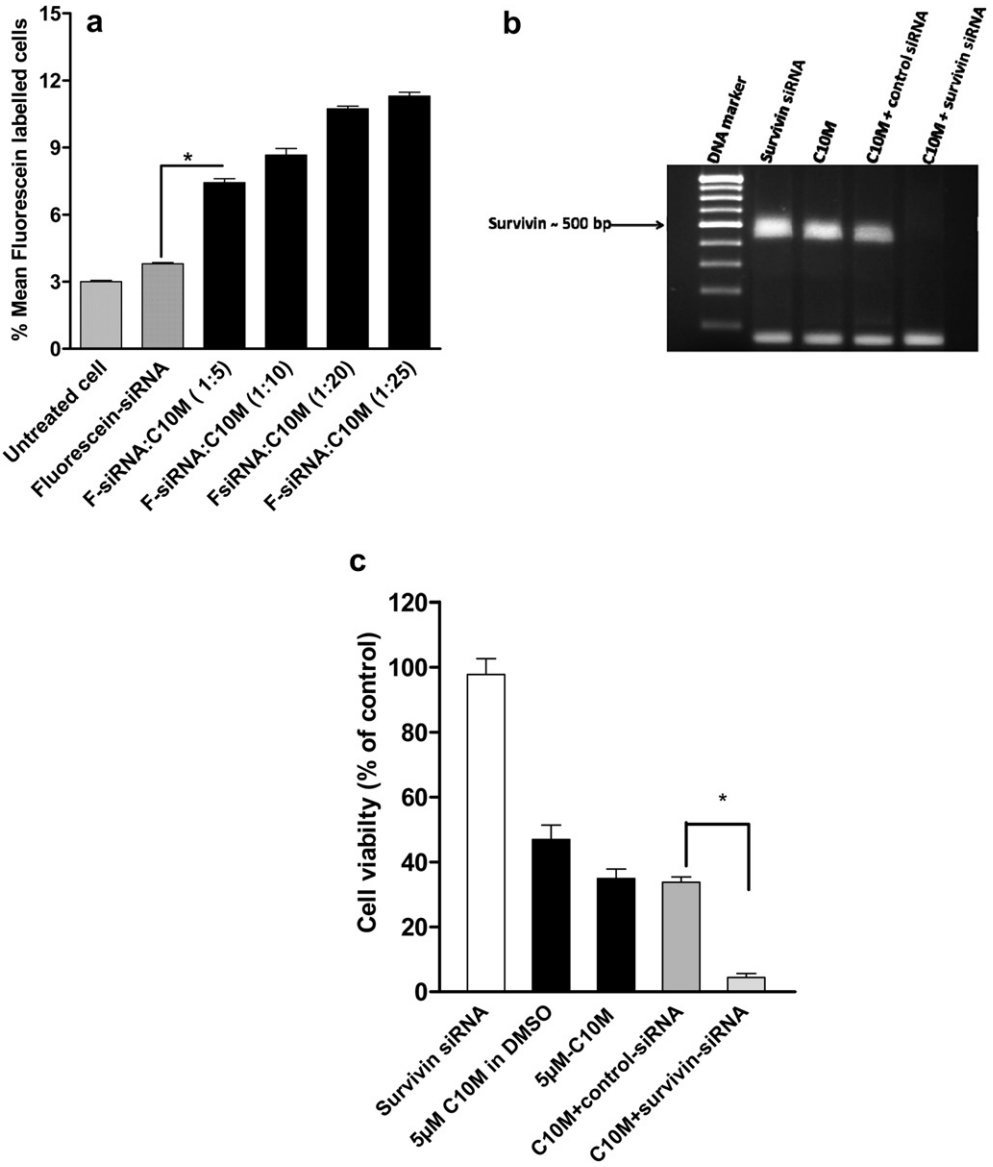

Fig. 2. siRNA transfection and combinational cell killing affect of anticancer siRNA and bifunctional lipo-benzamide. a) Cellular uptake, as determined by flow cytometry of Fluorescein-labeled siRNA and complexes formed with C10M compared to untreated DU-145 (control). Error bars represent the standard error of the mean. siRNA delivery efficacy of C10M in DU-145 is statistically significant, $^{*}p < 0.05$. b) Semi quantitative RT-PCR detection of endogenous survivin mRNA silencing in DU-145 cells by anticancer delivery vehicles. C10M transfection efficiency was measured using survivin siRNA and compared with controls. Only, Survivin-siRNA and C10M used as normal controls; C10M + control siRNA used as negative control. c) Combined *in vitro* antiproliferative activity of C10M: survivin siRNA (25:1 weight ratio) complex. Cells were treated with siRNA alone, C10M dissolved in DMSO, self assembled C10M, C10M control siRNA complex and C10M survivin siRNA complex for 12 h followed by replacement of the existing media with fresh media and further incubation for 12 h. Antiproliferative activity was assayed by MTT reagent. The *Y*-axis represents % viability. Each data point is the representation of triplicate treatments. *Represents $p < 0.05$.

2.3.2. Gene silencing efficiency of siRNA/C10M complex

To further demonstrate the endogenous gene silencing efficiency of the C10M/siRNA formulation, siRNA against survivin was delivered to the DU-145 cells and survivin mRNA levels were determined by semi-quantitative reverse transcription polymerase chain reaction (RT-PCR) analysis 24 h post-transfection. Briefly, 1.5×10^5 DU-145 cells were seeded in 6 well plates, after 80% confluence cells were treated either with 100 nM siRNA (control or survivin) or 100 nM siRNA + 2.5 μg C10M (1:25) complex for 12 h, after that siRNA and treatment containing media was carefully removed, fresh media was added and cells were further incubated for 24 h. DU-145 cells were treated with 100 nM of human survivin siRNA alone or complexed with 2.5 μg self assembled C10M (1:25, siRNA:lipid weight ratio) to provide a measure of target gene silencing at the mRNA level. To prepare lipoplex, 5 μL of, 1 mM self assembled C10M formulation was transferred to a 1.5 mL eppendorf tube and 95 μL of RPMI was added. To the resultant mixture, siRNA suspended in 100 μL of RPMI was added and the whole mixture incubated for 30 min. After incubation, 300 μL of RPMI containing 10% FBS were added to the resulting lipoplex for transfection experiments. Following 24 h of incubation with the lipoplex, cells were lysed and RNA isolated using Trizol reagent (Invitrogen, USA) as per the manufacturer's instructions. Total RNA was reverse transcribed by Super script III, (Invitrogen, USA) cDNA synthesis kit as per the manufacturer's instructions. Thereafter, RT-PCR was performed on survivin and 18 S ribosomal RNA using the Platinum® PCR SuperMix (Promega corporation, USA). The amplification conditions are described in Supporting information. The amplified sequences were resolved on a 1.4% agarose gel and visualized using 0.1%

ethidium bromide under UV light. The mRNA expression levels of survivin were decreased significantly by treatment with C10M survivin siRNA complexes, but the individual treatment of either siRNA or cationic compound and control siRNA C10M complex did not affect survivin levels (Fig. 2b).

2.3.3. Combined anticancer effect of anticancer lipid and siRNA

We tested the combined effect of anticancer siRNA and lipo-benzamide (C10M) on cancer cell killing using the MTT reduction assay. Five groups composed of 5×10^3 cells treated with either 100 nM survivin siRNA alone, 5 μM C10M in DMSO, 5 μM self assembled C10M, or 100 nM control or survivin siRNA complexed with 5 μM C10M complexed with 5 μM C10M were incubated with DU-145 cells for 12 h. Following incubation, siRNA and C10M containing media was carefully removed, fresh media was added and cells were further incubated for 24 h. Cultures were treated with 10 μL of MTT for a final 3 h, formazan solubilized with DMSO-methanol 1:1 and absorbance read at 540 nm. The data indicate that survivin siRNA delivered by C10M had significantly higher antiproliferative activity than C10M ($p < 0.05$) and control siRNA had no effect on cell survival (Fig. 2c). Further, free survivin siRNA did not induce any cytotoxicity due to the lack of spontaneous cellular entry. Interestingly, self assembled C10M had higher antiproliferative activity than its DMSO solution.

3. Conclusions

The present report describes the discovery of a novel bifunctional, cationic lipo-benzamide (C10M) which induces apoptosis selectively in prostate cancer cells similar to targeted anticancer agents and also self assembles and delivers siRNA. The compound is easy to synthesize and both the antiproliferative activity and siRNA delivery capability are highly efficient and consistent. To verify the potential of C10M as a combinational antitumor agent *in vivo*, we are currently pursuing the targeted delivery of anticancer siRNA and paclitaxel in mouse models of breast and prostate cancer. Our recent research effort is also focused toward the development of bifunctional cationic molecule (serving as both, a formulation component as well as a therapeutic agent) containing multifunctional nanoparticles to effectively treat cancer.

4. Experimental protocols

4.1. Biological methods

The size of the self assembled C10M was obtained from Malvern Instruments Zetasizer nano-ZS. The human cancer cell lines e.g. prostate cancer cells (PC-3 and DU-145), MCF-7, HepG2 and normal non-transformed cell types WPMY-1, NIH/3T3, COS-7 used in the present study were obtained from the ATCC (American Type Culture Collection, USA). Cell viability measurement kit (CCK-8), was purchased from the Dojinando Laboratories (Kumamoto, Japan). The sense 5′-fluorescein-modified siRNA duplex was obtained from Dharmacon. Sequence of 5′-fluorescein siRNA: Sense: 5′-CUU ACG CUG AGU ACU UCG AdTdT-3′, Antisense: 5′-UCG AAG UAC UCA GCG UAA GdTdT-3′. Control siRNAs, and survivin siRNA were procured from Sigma–Aldrich. Sequence of siRNA against human survivin: Sense: 5′-GGA CCA CCG CAU CUC UAC AdTdT-3′, Antisense: 5′-UGU AGA GAU GCG GUG GUC CdTdT-3′. Sequence of scrambled siRNA: Sense strand: 5′-ACGCGUAACGCGGGAAUUUdTdT3′ Antisense strand: 5′-AAAUUCCCGCGUUACGCGUdTdT-3′. All detailed procedures of biology experiments were included in Supporting information.

4.2. Statistical analysis

All data are expressed as mean ± SE. Differences between groups were explored using analysis of variance (ANOVA). Wherever the ANOVA indicated a significant difference, individual differences were explored using *t* tests with a Dunnett or Turkeys correlation multiple comparisons. Differences were considered statistically significant for at $^*p < 0.05$. All the statistical analysis was performed using Graph Pad Prism version 4.00 for Windows (Graph Pad Software, USA).

4.3. Chemical methods

4.3.1. Synthesis of the cationic lipo-benzamide derivatives

Scheme 1 outlines the synthetic strategy employed for preparing the cationic lipo-benzamide derivatives described in the present study. Detailed experimental procedure for the synthesis of C10M is delineated below.

*4.3.1.1. Synthesis of tert-butyl 2-(4-methoxybenzamido)ethyl-carbamate (**1**).* To a solution of *tert*-butyl 2-aminoethylcarbamate (2.01 g, 12.56 mmol) in a mixture of triethylamine (3.49 mL, 25.1 mmol) and THF (20 mL), anisoylchloride (1.93 mL, 14.25 mmol) was added drop wise and reaction mixture was stirred at room temperature for 3 h. After completion of the reaction whole reaction mixture was diluted with 50 mL of ethyl acetate, washed with water (1 × 50 mL), brine solution (1 × 50 mL) and finally dried with anhydrous sodium sulfate. Column chromatographic purification (using 60–120 mesh silica gel and 4% methanol in chloroform as eluting solvent mixture) of the residue afforded **1** (Scheme 1) (1.7 g, 46% yield, R_f: 0.8 in 10% methanol in chloroform).

^{1}H NMR (200 MHz, $CDCl_3$) δ = 1.39 [m, 9H{NHCOOC(CH_3)$_3$}], 3.08–3.2 {m, 2H($NH_2CH_2CH_2$)}, 3.3–3.4 {m, 2H($NH_2CH_2CH_2$)}, 3.85 {s, 3H(OCH_3)}, 6.9–7.13 {m, 2H(m-Ph)}, 7.74–7.8{m, 2H(o-Ph)}, 8.32 {s, 1H(CH_2CH_2NH)}.

FABMS: *m*/*z*: 295 $(M + H)^+$.

*4.3.1.2. Synthesis of N-(2-didecylamino-ethyl)-4-methoxy-benzamide (**2**).* Product obtained in the above step was dissolved in (**1**, 1.7 g, 1.78 mmol) a 1:1 mixture of trifluoroacetic acid and dichloromethane. The reaction mixture was stirred at room temperature for 90 min. TFA was removed under reduced pressure by co-evaporating with toluene. Column chromatographic purification (using 60–120 mesh silica gel and 8% methanol in chloroform as eluting solvent mixture) of the dried residue afforded primary amine derivative (0.67 g, 66% yield, R_f: 0.4 in 10% methanol in chloroform).

To, ethyl acetate (10 mL) solution of above free amine derivative (0.67 g, 3.45 mmol) K_2CO_3 (2.34 g, 13.8 mmol) and 1-decyl bromide (1.82 mL, 8.8 mmol) were added. The whole mixture was refluxed at 70 °C for 12 h. After completion of the reaction, the reaction mixture further diluted with 20 mL of ethyl acetate and washed with water (2 × 20 mL). The organic layer dried with anhydrous Na_2SO_4 and concentrated in vacuum. Column chromatographic purification (using 60–120 mesh silica gel and 35% ethyl acetate in hexane as eluting solvent) of the residue afforded alkylated benzamides **2** (Scheme 1) (0.73 g, 45% yield, R_f: 0.4 in 10% methanol in chloroform).

N-(2-Didecylamino-ethyl)-4-methoxy-benzamide: Yield: 45%.

^{1}H NMR N-(2-didecylamino-ethyl)-4-methoxy-benzamide (300 MHz, $CDCl_3$) δ = 0.87 [t, 6H, *J* = 6.62 Hz, {N(CH_2)$_9$$CH_3$}]; 1.14–1.37 [m, 28H {$NCH_2CH_2$($CH_2$)$_7$$CH_3$}]; 1.63–1.74 [m, 4H, {$NCH_2CH_2$($CH_2$)$_7$$CH_3$}]; 2.44 [t, 4H, *J* = 7.19 Hz, {NCH_2CH_2(CH_2)$_7$$CH_3$}]; 2.62 {t, 2H, *J* = 5.46 Hz, (NCH_2CH_2)}; 3.46 {q, 2H,

J = 5.52 Hz, ($NC\underline{H}_2CH_2$)}; 3.84 {s, 3H, ($OC\underline{H}_3$)}; 6.89–6.91 {m, 3H, (m-Ph & NH)}; 7.74 {d, 2H, J = 8.85 Hz, (o-Ph)}.

ESIMS: m/z: 475 $(M + H)^+$.

4.3.1.3. Synthesis of didecyl-[2-(4-methoxy-benzoylamino)-ethyl]-methyl-ammonium iodide (C10M). To the tertiary benzamide obtained from above step (**2**, 0.73 g, 1.54 mmol) in DCM (5 mL), methyl iodide (15–20 equivalents) was added. The reaction mixture was stirred at room temperature for 3 h. Solvent was removed under vacuum. Column chromatographic purification (using 60–120 mesh silica gel and 30% acetone in hexane as eluting solvent) of the residue afforded quaternary benzamide C10M (Scheme 1 representative structure indicated as **CM**) as a solid materials (0.628 g, 83.5% Yield, R_f: 0.71 in 60% acetone in hexane).

^{1}H NMR (300 MHz, $CDCl_3$) δ = 0.87 [t, 6H, {$N(CH_2)_9CH_3$}]; 1.13–1.37 [m, 28H, {$NCH_2CH_2(CH_2)_7CH_3$}]; 1.63–1.72 [m, 4H, {$NCH_2CH_2(CH_2)_7CH_3$}]; 3.28 {s, 3H, ($N + CH_3$)}; 3.43–3.48 [m, 4H, {$NCH_2CH_2(CH2)_7CH_3$}]; 3.81–3.84 {m, 5H, (OCH_3 & NCH_2CH_2)}; 3.99 {d, 2H, J = 4.32 Hz, (NCH_2CH_2)}; 6.92 {d, 2H, J = 8.75 Hz, (m-Ph)}; 8.07 {d, 2H, J = 8.84 Hz, (o-Ph)}; 8.53 {t, 1H, J = 5.4 Hz, ($NHCH_2CH_2$)}.

^{13}C NMR (300 MHz, CDCl3) δ = 167.7, 162.6, 129.6, 124.8, 113.7, 62.8, 60.5, 55.3, 49.4, 34, 31.8, 29.3, 29.2, 29.1, 26.2, 22.6, 22.5, 14.

ESIMS: m/z: 489 $(M)^+$.

IR (KBr) values: 3282.3, 2925.4, 2855.2, 1652.3, 1535.7, 1254.3, 1038.2, 844.2, 769.1, 603 cm^{-1}.

HRMS (ESI) calculated for $C_{31}H_{57}N_2O_2$: 489.7899 found = 489.4486.

M.P: 120–122 °C.

Other alkyl chain derivatives are prepared following the same procedure and the details of the ^{1}H NMR chemical shifts and molecular ion peaks were included in Supporting information.

Acknowledgments

Instrumentation facilities from SAIF, CDRI are gratefully acknowledged. This is CDRI–CSIR communication and Prathap Reddy and R.K.G. thanks Council of Scientific Industrial Research (CSIR), Government of India for a Ph.D. fellowship. Komal Sharma thanks Department of Science and Technology (DST) for the INSPIRE fellowship. Durga Prasad Mishra acknowledges financial assistance from Ministry of Health, Government of India in form of a grant 'GAP-0001'. Surendar Reddy Bathula acknowledges financial assistance from CSIR, in a form of EMPOWER project. Amit Misra's help in manuscript preparation is acknowledged.

Appendix A. Supporting information

Supporting information related to this article can be found online at http://dx.doi.org/10.1016/j.ejmech.2012.07.035.

References

[1] (a) K.A. Whitehead, R. Langer, D.G. Anderson, Nat. Rev. Drug Discov. 8 (2009) 129–138;
(b) K. Gao, L. Huang, Mol. Pharm. 6 (2009) 651.
[2] J.C. Burnett, J.J. Rossi, K. Tiemann, Biotechnol. J. 6 (2011) 1130–1146.
[3] S.C. Semple, A. Akinc, J. Chen, A.P. Sandhu, B.L. Mui, C.K. Cho, D.W. Sah, D. Stebbing, E.J. Crosley, E. Yaworski, I.M. Hafez, J.R. Dorkin, J. Qin, K. Lam, K.G. Rajeev, K.F. Wong, L.B. Jeffs, L. Nechev, M.L. Eisenhardt, M. Jayaraman, M. Kazem, M.A. Maier, M. Srinivasulu, M.J. Weinstein, Q. Chen, R. Alvarez, S.A. Barros, S. De, S.K. Klimuk, T. Borland, V. Kosovrasti, W.L. Cantley, Y.K. Tam, M. Manoharan, M.A. Ciufolini, M.A. Tracy, A. de Fougerolles, I. MacLachlan, P.R. Cullis, T.D. Madden, M.J. Hope, Nat. Biotechnol. 28 (2010) 172–176.
[4] B.L. Davidson, P.B. McCray Jr., Nat. Rev. Genet. 12 (2011) 329–340.
[5] D. Strumberg, B. Schultheis, U. Traugott, C. Vank, A. Santel, O. Keil, K. Giese, J. Kaufmann, J. Drevs, Int. J. Clin. Pharmacol. Ther. 50 (2012) 76–78.
[6] M.E. Davis, J.E. Zuckerman, C.H. Choi, D. Seligson, A. Tolcher, C.A. Alabi, Y. Yen, J.D. Heidel, A. Ribas, Nature 464 (2010) 1067–1070.
[7] M. Scherr, K. Battmer, T. Winkler, O. Heidenreich, A. Ganser, M. Eder, Blood 101 (2003) 1566–1569.
[8] S.D. Li, L. Huang, Ann. N. Y. Acad. Sci. 1082 (2006) 1–8.
[9] R. Srinivas, S. Samanta, A. Chaudhuri, Chem. Soc. Rev. 38 (2009) 3326–3338.
[10] (a) M. Nothisen, M. Kotera, E. Voirin, J.S. Remy, J.P. Behr, J. Am. Chem. Soc. 131 (2009) 17730–17731;
(b) O. Nakagawa, X. Ming, L. Huang, R.L. Juliano, J. Am. Chem. Soc. 132 (2010) 8848–8849.
[11] D. Lane, Nat. Biotechnol. 24 (2006) 163–164.
[12] L. Huang, Y. Liu, Annu. Rev. Biomed. Eng. 13 (2011) 507–530.
[13] (a) G. Wang, C. Kucharski, X. Lin, H. Uludağ, J. Drug Target. 18 (2010) 611;
(b) M. Ogris, S. Brunner, S. Schüller, R. Kircheis, E. Wagner, Gene Ther. 6 (1999) 595–605.
[14] J. Gao, W. Liu, Y. Xia, W. Li, J. Sun, H. Chen, B. Li, D. Zhang, W. Qian, Y. Meng, L. Deng, H. Wang, J. Chen, Y. Guo, Biomaterials 32 (2011) 3459–3470.
[15] Y. Chen, J. Sen, S.R. Bathula, Q. Yang, R. Fittipaldi, L. Huang, Mol. Pharm. 6 (2009) 696–705.
[16] Y. Chen, S.R. Bathula, J. Li, L. Huang, J. Biol. Chem. 285 (2010) 22639–22650.
[17] Y. Chen, S.R. Bathula, Q. Yang, L. Huang, J. Invest. Dermatol. 130 (2010) 2790–2798.
[18] S. Sinha, S. Roy, S.R. Bathula, K. Pal, G. Sudhakar, S. Iyer, S. Dutta, E. Wang, P.K. Vohra, K.R. Roy, P. Reddanna, D. Mukhopadhyay, R. Banerjee, Mol. Cancer Res. 9 (2011) 364–374.
[19] K. Pal, S. Pore, S. Sinha, R. Janardhanan, D. Mukhopadhyay, R. Banerjee, J. Med. Chem. 54 (2011) 2378–2390.
[20] R. Banerjee, P. Tyagi, S. Li, L. Huang, Int. J. Cancer 112 (2004) 693–700.
[21] M.F. Moreau, J. Michelot, J. Papon, M. Bayle, P. Labarre, J.C. Madelmont, D. Parry, J.Y. Boire, N. Moins, H. Seguin, Nucl. Med. Biol. 22 (1995) 731–741.
[22] (a) G.Y. Miao, Q.M. Lu, X.L. Zhang, World J. Gastroenterol. 13 (2007) 1170–1174;
(b) X. Liu, R. Gao, Y. Dong, L. Gao, Y. Zhao, L. Zhao, X. Zhao, H. Zhang, BMC Cancer 10 (2010) 1–13;
(c) H. Caldas, L.E. Honsey, R.A. Altura, Mol. Cancer 4 (2005) 1–9;
(d) D.C. Altieri, Oncogene 22 (2003) 8581–8589;
(e) D.C. Altieri, Cancer Lett., in press.
[23] I. Vermes, C. Haanen, H. Steffens-Nakken, C. Reutelingsperger, J. Immunol. Methods 184 (1995) 39–51.
[24] M.F. Tsou, H.F. Lu, S.C. Chen, L.T. Wu, Y.S. Chen, H.M. Kuo, S.S. Lin, J.G. Chung, Anticancer Res. 26 (2006) 1965–1972.
[25] J.K. Buolamwini, Curr. Pharm. Des. 6 (2000) 379–392.
[26] J. Sridhar, N. Akula, N. Pattabiraman, AAPS J. 8 (2006) E204–E221.
[27] (a) T. Hashimoto, Z. He, W.Y. Ma, P.C. Schmid, A.M. Bode, C.S. Yang, Z. Dong, Cancer Res. 1 (2004) 3344–3349;
(b) W. Qi, D. Qiao, J.D. Martinez, Radiat. Res. 157 (2002) 166–174;
(c) M.H. Lee, H.Y. Yang, Cancer Metastasis Rev. 22 (2003) 435–449.
[28] Glide, Version 5.5, Schrödinger, Inc., New York, NY, 2009.